**IOSR Journal of Engineering (IOSRJEN)** **www.iosrjen.org**
ISSN (e): 2250-3021, ISSN (p): 2278-8719
PP 40-47

# Autism Spectrum Disorder Detection in Children Using Adaptive Kalman Filtering Approach

D.Umanandhini[1], Dr.G.Kalpana[2].
[1]*Research Scholar Departemnt of computer science, Sri Ramakrishna College Of Arts And Science For Women ,Coimbatore-46*
[2]*Associate Professor, Departemnt of computer science, Sri Ramakrishna College Of Arts And Science For Women , Coimbatore-46*

***Abstract:*** *This research work aims to design and develop an adaptive kalman filter in physiological detection of anxiety related arousal in children those who are having autism spectrum disorder (ASD). Unlike classical adaptive Kalman filters, which have been designed for state estimation in case of uncertainties about noise covariances, the adaptive Kalman filter proposed in this paper is for the purpose of ASD classification, through joint state-parameter estimation. The stability and minimum variance properties of the adaptive Kalman filter have been implemented. In this part of research work, a stochastic framework, with rigorously established statistical and stability properties. In particular, it is shown that the proposed adaptive Kalman filter provides a recursive estimation of actuator fault parameters equivalent to the recursive least squares estimator formulated for a fictive regression problem. From the results it is proved that the proposed adaptive kalman filter performs better in terms of sensitivity, specificity, fallout rate, miss rate, accuracy and time.*
***Keywords:*** *kalman filter, autism spectrum disorder, ASD, sensitivity, specificity, fall out, miss rate, accuracy.*

## I. INTRODUCTION

Anxiety is a condition of worried expectation and is related with increased pressure, excitement, and negative valence. Programmed discovery of anxiety has gotten consideration in a few fields including human-PC cooperation, savvy transport frameworks, security and access control, workload evaluation, and wellbeing observing. All the more as of late, programmed discovery of anxiety has been proposed as a way to give a target measure that can supplement clinical anxiety treatment programs. Truth be told, administration of physiological side effects is an indispensable piece of existing medicines. These projects, be that as it may, depend on the person's capacity to self-reflect and self-perceive physiological indications of anxiety and are not appropriate to the necessities of clinical populaces who have scholarly handicap or potentially deficiencies in correspondence, thoughtfulness, and passionate mindfulness. A case of such populace is people with autism spectrum disorder (ASD). ASD is a pervasive and complex neuro-formative disorder portrayed by subjective weaknesses in social correspondence, and by the nearness of prohibitive and dreary practices as well as premiums. Anxiety is a common, diligent, and impairing co-bleakness in ASD. Notwithstanding its significant negative effect on physical and psychological wellness, anxiety communicates with the center deficiencies of ASD to compound symptomatology and increment practical hindrance. Notwithstanding the direness to treat co-sullen anxiety in ASD, there is constrained proof supporting treatment programs in higher-working people, and no confirmation for the individuals who are bring down working. Key ASD-related hindrances to anxiety treatment are weaknesses in psychological capacity, correspondence, passionate mindfulness, and reflection.

## II. LITERATURE REVIEW

The mix of machine-learning strategies with mind imaging information has took into consideration the classification of mental states related with the portrayal of semantic classifications (Haxby, 2001; O'Toole et al., 2005), of the implications of things (Buchweitz et al., 2012; Mitchell et al., 2008; Shinkareva et al., 2011), of feelings (Kassam et al., 2013), and of learning (Bauer and Just, 2015). On account of mental illness states, thinks about have recognized patients of cerebrum enactment related with schizophrenia (Yang et al., 2010), with a mental imbalance (Just et al., 2014), and with sorrow (Craddock et al., 2009). Concentrates that connected ML calculations to ASD mind imaging information have characterized people as extremely introverted or control from their fMRI cerebrum actuation with up to 97% precision inside single destinations. They additionally recognized an example of cerebrum enactment related with a mental factor (self-portrayal). The example was available in control patients and almost truant for extremely introverted members (Just et al., 2014). In another investigation of classification of ASD members (Plitt et al., 2015), the creators acquired a 76.67% classification exactness in a populace test of 178 ASD and IQmatched ordinarily creating members. A proviso of concentrates that connected supervised ML to cerebrum imaging information is their generally

modest number of members. Arbabshirani et al. (2016) demonstrated that the solid classification exactnesses of ML ponders were gotten with populace tests with less than 100 members; higher classification correctnesses, that is, over 90%, were just acquired with thinks about compelled to many members. Classification precision drops fundamentally in bigger populace tests and if information is from various destinations (Nielsen et al., 2013). Most investigations that consolidate mind imaging and machine learning have connected supervised learning strategies, for example, support vector machine (SVM) or Gaussian Naive Bayes (GNB) classifiers. The subjectivity of highlight choice strategies for supervised machine learning techniques might be an obstruction for the correlation of results crosswise over examinations. In supervised strategies, class names are allotted to an arrangement of information utilized as the preparation informational collection; other information focuses (test informational index) are grouped in connection to the examples found in the preparation information (utilizing the given marks). At the end of the day, the calculation works to order pre-set up marks (that is, they depend on include choice, or highlight building). The decision of these marks and of the highlights relies upon from the earlier theory or exploratory methodology; henceforth, they rely upon a level of subjectivity. For instance, the quantity of voxels utilized for classification of mind imaging information has been exactly chosen based on investigating sets of 100, 200, 400 and more voxels and recognizing the set size that works best for the classification (Buchweitz et al., 2012; Mitchell et al., 2008; Shinkareva et al., 2011).

Koyamada et al. (2015) explored brain states from quantifiable brain exercises by utilizing Deep Neural Networks (DNN). They prepared an counterfeit neural system with two hidden layers and a softmax yield layer to classify errand based fMRI information from 499 subjects into seven classifications identified with the assignments: Emotion, Gambling, Language, Motor, Relational, Social and Working Memory. Deep models took into account better outcomes (mean accuracy of 50.74%) contrasted with directed learning techniques (mean accuracy of 47.97%, for example, Linear Regression what's more, Support Vector Machine. Plis et al. (2014) utilized deep learning and auxiliary T1-weighted pictures keeping in mind the end goal to classify patients with schizophrenia versus coordinated solid controls, utilizing information from four extraordinary destinations; the creators likewise arranged patients with Huntington ailment versus sound controls, utilizing information joined by the PREDICT-HD venture (www.predict-hd.net). To begin with, they endeavored to classify 198 schizophrenic patients and 191 controls from four distinct examinations directed by Johns Hopkins University (JHU), the Maryland Psychiatric Research Center (MPRC), the Institute of Psychiatry, London, UK (IOP), and the Western Psychiatric Institute and Clinic at the University of Pittsburgh (WPIC). Plis et al. prepared a Deep Belief Network with 3 profundities (50 hidden units in the main layer, 50 in the second layer, and 100 in the best layer). They accomplished 90% characterization accuracy utilizing highlights separated from three DBMs in contrast with 68% characterization accuracy utilizing crude information in a Support Vector Machine. The creators reasoned that deep learning holds awesome potential for clinical brain applications.

## III. ADAPTIVE KALMAN FILTER

In the Adaptive Kalman Filter, the state evaluate $\hat{x}(k|k) \in \mathbb{R}^p$and the parameter assess $\bar{\theta}(k) \in \mathbb{R}^p$are recursively refreshed at each time moment $k$. This algorithm includes likewise a couple of other recursively refreshed auxiliary factors: $P(k|k) \in \mathbb{R}^{n-n}, Y(k) \in \mathbb{R}^{n-p}, S(k) \in \mathbb{R}^{p-p}$and an overlooking element $\lambda \in (0,1)$. At the underlying time moment $k = 0$, the underlying state $x(0)$ is assumed to be a Gaussian random vector $x(0) \sim N(x_0, P_0)$.Considering $\theta_0 \in \mathbb{R}^p$ a chance to be the underlying estimate of $\theta, \lambda \in (0,1)$ is picked overlooking component, and ω be a picked positive incentive for initializing$S(k)$, at that point the flexible Kalman channel comprises of the introduction step and the recursion steps depicted underneath.

### 3.1. Stability of the adaptive Kalman filter

The primary motivation behind this segment is to demonstrate that the mathematical desires for the state and parameter estimation blunders tend exponentially to zero when $k \to \infty$. In other words, the deterministic piece of the mistake progression framework is exponentially steady. Another reason for this segment is to demonstrate

that the recursively processed networks $P(k|k), \Upsilon(k), S(k)$ are altogether limited, so are the state and parameter estimation pick up frame works $K(k)$ *and* $\Gamma(k)$.

Considering the frameworks $A(k), B(k), C(k), \Phi(k), Q(k), R(k)$ and the information $u(k)$ are upper limited, $Q(k)$ is symmetric positive semi clear, and $R(k)$ is symmetric positive-distinct with an entirely positive lower headed, for all $k \geq 0$. For controlled frameworks, boundedness is normally guaranteed by controllers; specifically the information can be immersed or compelled, as on account of Model Predictive Control (MPC).

Considering the $[A(k), C(k)]$ combine is consistently totally discernible, and the $[A(k), Q^{\frac{1}{2}}(k)]$ match is consistently totally controllable, in the feeling of the uniform positive definiteness of the relating Gramian frameworks. (Jazwinski, 1970; Kalman,1963). As the absence of recognizability as well as controllability relates to non-negligible state space models, it can be kept away from by utilizing insignificant state space models.

Considering the signs contained in the matrix $\Phi(k)$ are relentlessly energizing as in there exist a number $h > 0$ and a genuine steady $\alpha > 0$ to such an extent that, for all integer $k \geq 0$, the matrix sequence $\Omega(k)$ driven by $\Phi(k)$ through the straight framework, fulfills

$$S\sum_{s=0}^{h-1} \Omega^T(k+s)\Sigma^{-1}(k+s)\Omega(k+s) \geq \alpha I_p \quad (1)$$

The age of $\Omega(k)$ can be seen as a direct filter in state-space shape, filtering the signs contained in the matrix $\Phi(k)$. At the point when the vector θ has close to segments than yield sensors, i.e., $p \leq m$, the matrix $\Omega(k) \in \mathbb{R}^{m-p}$ has no a larger number of sections than lines, then each term on the whole is commonly of full rank. At the point when $p > m$, Assumption 3 implies that the signs contained in $\Phi(k)$ must change adequately finished the time. On account of time in variation frameworks (with consistent grids A, C, K), like the classical steady excitation conditions for framework recognizable proof or parameter estimation (Ljung, 1999), Assumption 3 infers an adequate number of recurrence segments in the signs contained in $(k)$.

**3.2. Minimum covariance of combined estimation errors**

The accompanying outcome is a speculation of the minimum fluctuation property of the classical Kalman filter. In the adaptive Kalman filter (5), relax the Kalman gain $K(k)$ are calculated through the intermittent conditions to any matrix grouping $L(k) \in \mathbb{R}^{n-m}$.

Considering the combined state and parameter estimation blunder $\xi(k) = \tilde{x}(k|k) - \Upsilon(k)\tilde{\theta}(k)$. Its covariance matrix relying upon the pick up arrangement L(k) and signified by $ov[\xi(k)|L]$ achieves its minimum when $L(k) = K(k)$, in the sense of the positive definiteness of the distinction matrix:

$$cov[\xi(k)|L] - cov[\xi(k)|K] \geq 0 \quad for\ any\ L(k) \in \mathbb{R}^{n-m} \quad (2)$$

This outcome implies that $v^T\, cov[\xi\,(k)|L]v \geq v^T\, cov[\xi\,(k)|K]v$ for any vector $v \in \mathbb{R}^n$. Truth be told, the term $\Upsilon\,(k)\tilde{\theta}\,(k)$ is the piece of the state estimation blunder $\tilde{x}(k|k)$ because of the parameter estimation error $\tilde{\theta}(k)$ (this part would be zero if the parameter assess $\hat{\theta}\,(k)$was supplanted by the genuine parameter esteem θ, and after that the adaptive Kalman filter would be lessened to the standard Kalman filter). Therefore, the significance of this proposition is that the rest of the piece of the state estimation mistake achieves its minimum change if the Kalman pick up $K(k)$ is utilized.

### 3.3. Equivalence to recursive least squares parameter estimator

The accompanying proposition expresses that the parameter estimation inside the adaptive Kalman filter is proportional to the classical recursive least squares (RLS) estimation defined for an imaginary relapse issue.

The linear regression is denoted as

$$z(k) = \Omega(k)\theta + \varepsilon(k) \quad (3)$$

where

- the matrix of relapses $\Omega(k) \in \mathbb{R}^{m-p}$,
- the relapse parameter vector $\theta \in \mathbb{R}^p$is equivalent to the vector θ showing up in the term $\Phi(k)\theta$ of framework,
- the mistake term $\varepsilon(k) \in \mathbb{R}^m$ is equivalent to the development grouping of the standard Kalman filter connected to the fault free (θ = 0) system, which is a white Gaussian clamor with its covariance matrix Σ(k).

Then the RLS assess $\hat{\theta}_{RLS}\,(k)$ for the straight relapse is indistinguishable to the parameter evaluate $\hat{\theta}(k)$, i.e., $\hat{\theta}_{RLS}\,(k) = \hat{\theta}\,(k)\, for\, all\, k \geq 0$, gave the two algorithms are suitably instated and utilize the same overlooking variable $\lambda$.

The classical RLS estimator (see, e.g., Ljung, 1999) applied to the linear regression (3) is

$$\Lambda(k) = [\lambda\Sigma(k) + \Omega(k)S(k-1)\Omega^T\,(k)]^T \quad (4)$$

$$\Gamma\,(k) = S(k-1)\Omega^T\,(k)\Lambda(k) \quad (5)$$

$$S(k) = \frac{1}{\lambda}\, S(k-1) - \frac{1}{\lambda} S(k-1)\Omega^T\,(k)\Lambda(k)\Omega(k)S(k-1) \quad (6)$$

$$\hat{\theta}_{RLS}(k) = \hat{\theta}_{RLS}(k-1) + \Gamma\,(k)[z(k) - \Omega(k)\hat{\theta}_{RLS}(k-1)] \quad (7)$$

with the initial values $\hat{\theta}_{RLS}(0) = \theta_0$ and $S(0) = \omega I_p$, Because $\Omega(k), \Sigma(k)\ and\ \lambda$ are the same, so are $\Lambda(k), S(k)\ and\ \Gamma\,(k)$ computed with identical formulas (the initial value $S(0) = \omega I_p$ is also assumed identical).

Defining $\hat{\theta}_{RLS}(k) \triangleq \theta - \hat{\theta}_{RLS}(k)$, leads to

$$\hat{\theta}_{RLS}(k) = \hat{\theta}_{RLS}(k-1) - \Gamma(k)[z(k) - \Omega(k)\hat{\theta}_{RLS}(k-1)] \quad (8)$$

Substituting $z(k)$ with (8), then

$$\hat{\theta}_{RLS}(k) = \hat{\theta}_{RLS}(k-1) - \Gamma(k)[\Omega(k)\hat{\theta}_{RLS}(k-1) + \varepsilon(k)]$$

$$\tilde{\theta}_{RLS}(k) = [I_p - \Gamma(k)\Omega(k)]\tilde{\theta}_{RLS}(k-1) - \Gamma(k)\varepsilon(k). \quad (9)$$

Then again, for the adaptive Kalman filter, the parameter appraise mistake $\tilde{\theta}(k)$ was characterized, and it was indicated that $\tilde{\theta}(k)$ fulfills the repetitive condition, which is like (9). Moreover, it has been picked that $\hat{\theta}(0) = \hat{\theta}_{RLS}(0) = \theta_0$, $\tilde{\theta}(0) = \hat{\theta}_{RLS}(0)$. Therefore $\tilde{\theta}(k) = \hat{\theta}_{RLS}(k)$ for all $k \geq 0$. As $\tilde{\theta}(k) = \theta - \tilde{\theta}(k)$ *and* $\hat{\theta}_{RLS}(k) = \theta - \hat{\theta}_{RLS}(k)$ it is then inferred that $\hat{\theta}(k) = \hat{\theta}_{RLS}(k)$ for all $k \geq 0$. This result permits to surely know the pretended by the overlooking component $\lambda$.

## IV. RESULTS AND DISCUSSIONS

### 4.1 Performance Metrics:

- ✓ Sensitivity: It is the measure of proportion of actual positives that are correctly identified.
- ✓ Specificity: It is the measure of proportion of actual negatives that are correctly identified.
- ✓ Accuracy: It is the measure of proportion of true results (both true positives and true negatives) among the total number of cases examined.
- ✓ Fallout Rate: It is the measure between the number of negative events wrongly categorized as positive and the total number of actual negative events.
- ✓ Miss Rate: It is the measure of incorrect results that are, in fact, positive.
- ✓ Delay: It is the measure of time taken by classifier to give results.

### 4.2 About the Dataset

The information for building the dataset consumed around six months of time. The dataset contains 1499 patients records. For the confidentiality reasons, the name of the patient is not obtained. Out of 1499, 998 children are having the possibility of getting ASD and remaining don't have. The results are presented in Table. 1. From the Fig.1 - Fig. 5 it can be observed that the proposed Adaptive Kalman Filtering (AKFA) approach performs better than that of existing KF approach, where this research work used MATLAB R2013a for evaluation purpose.

| **METRICS** | **Existing - Kalman Filter Approach** | **Proposed - Adaptive Kalman Filter Approach** |
|---|---|---|
| TP | 957 | 986 |
| TN | 469 | 476 |
| FP | 39 | 20 |
| FN | 34 | 17 |
| Sensitivity (or) True Positive Rate **(%)** | 96 | 98 |
| Specificity (or) True negative Rate **(%)** | 92 | 95 |
| Fall - Out **(%)** | 8 | 4 |
| Miss rate **(%)** | 3 | 2 |
| **Accuracy (%)** | 95 | 97 |
| **Delay (s)** | 4.01 seconds | 3.82 seconds |

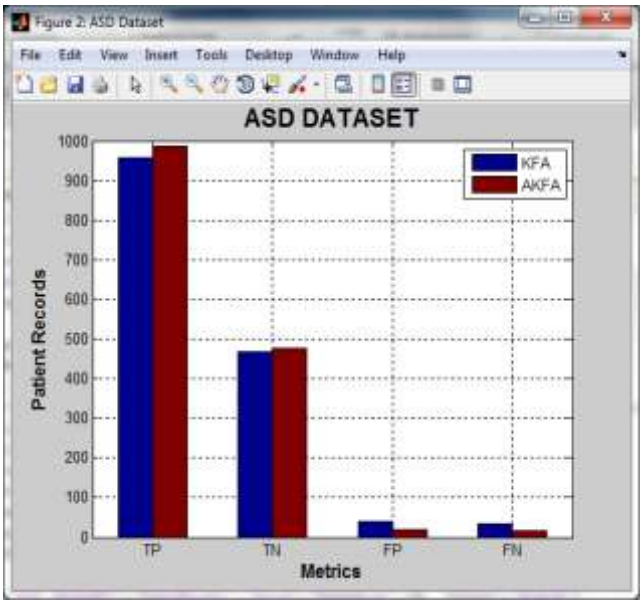


**Fig.1. TP, TN, FP, FN Analysis**

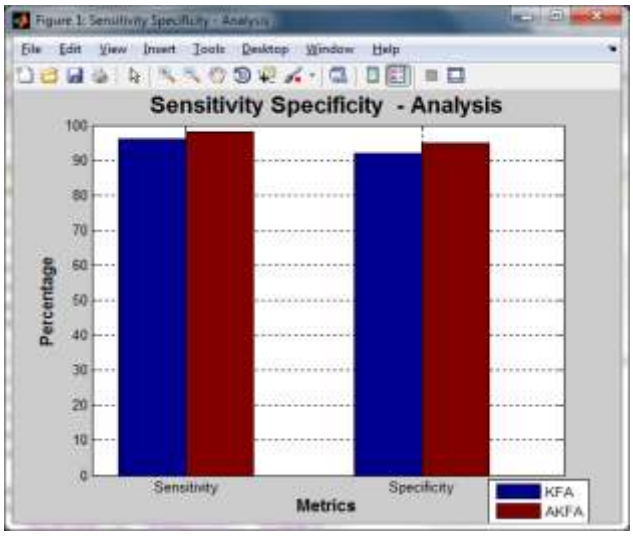


**Fig.2. Sensitivity and Specificity Analysis**

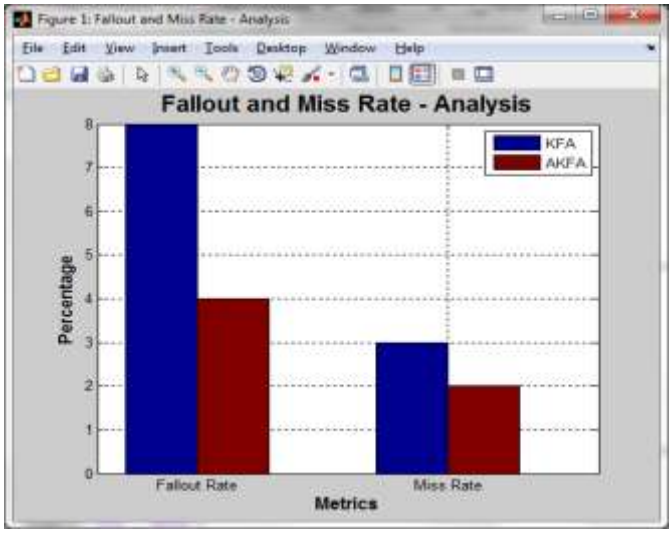


**Fig.3. Fall Out and Miss Rate Analysis**

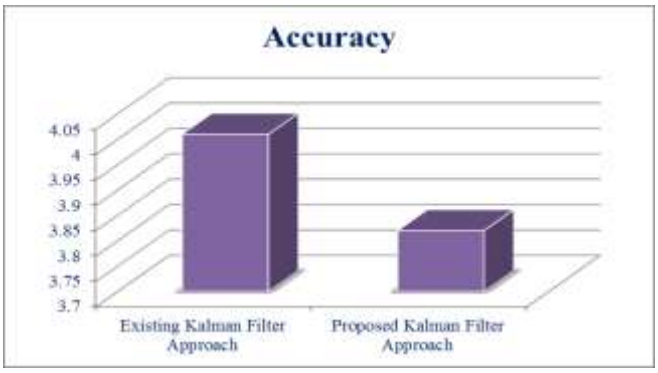


**Fig.4. Accuracy**

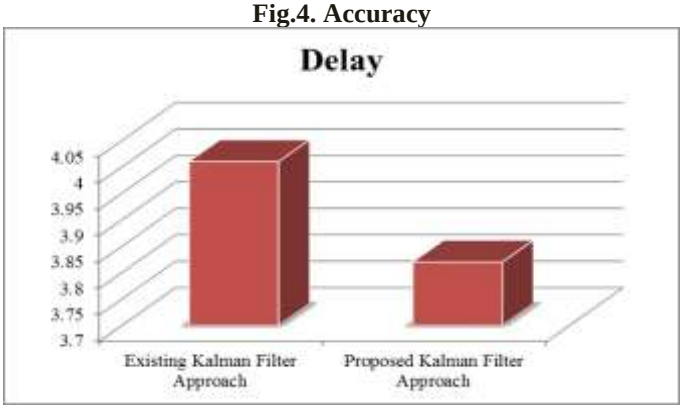


**Fig. 5. Delay Analysis**

## V. CONCLUSIONS

This paper presented an adaptive kalman filter in physiological detection of anxiety related arousal in children those who are having autism spectrum disorder (ASD). Not like conventional Kalman filters, which have been designed for state estimation in case of uncertainties about noise covariances, the adaptive Kalman filter proposed in this paper is for the purpose of ASD classification, through joint state-parameter estimation. The stability and minimum variance properties of the adaptive Kalman filter have been implemented. In this part of research work, a stochastic framework, with rigorously established statistical and stability properties. In particular, it is shown that the proposed adaptive Kalman filter provides a recursive estimation of actuator fault parameters equivalent to the recursive least squares estimator formulated for a fictive regression problem. From the results it is proved that the proposed adaptive kalman filter performs better in terms of sensitivity, specificity, fall out, miss rate, accuracy and time.

## REFERENCES

[1]. Abraham, A., et al., 2017. Deriving reproducible biomarkers from multi-site resting-state data: an autism-based example. NeuroImage 147, 736–745.
[2]. Akshoomoff, N., Corsello, C., Schmidt, H., 2006. The role of the autism diagnostic observation schedule in the assessment of autism spectrum disorders in school and community settings. Calif. Sch. Psychol. 11 (1), 7–19.
[3]. Altman, D.G., Bland, J.M., 1994. Diagnostic tests 2: predictive values. BMJ 309 (6947), 102. Anderson, J.S., et al., 2011. Functional connectivity magnetic resonance imaging classification of autism. Brain 134 (12), 3739–3751.
[4]. Arbabshirani, M.R., Plis, S., Sui, J., Calhoun, V.D., 2016. Single subject prediction of brain disorders in neuroimaging: promises and pitfalls. NeuroImage 145 (Pt B), 137–165.
[5]. Aylward, E.H., et al., 1999. MRI volumes of amygdala and hippocampus in non-mentally retarded autistic adolescents and adults. Neurology 53 (9) (2145–2145).
[6]. Bauer, A.J., Just, M.A., 2015. Monitoring the growth of the neural representations of new animal concepts. Hum. Brain Mapp. 36 (8), 3213–3226.
[7]. Behzadi, Y., Restom, K., Liau, J., Liu, T.T., 2007. A component based noise correction method (CompCor) for BOLD and perfusion based fMRI. NeuroImage 37 (1), 90–101.
[8]. Biswal, B., Yetkin, F.Z., Haughton, V.M., Hyde, J.S., 1995. Functional connectivity in the motor cortex of resting human brain using echo-planar MRI. Magn. Reson. Med. 34 (4), 537–541.
[9]. Buchweitz, A., Shinkareva, S.V., Mason, R.A., Mitchell, T.M., Just, M.A., 2012. Identifying bilingual semantic neural representations across languages. Brain Lang. 120 (3), 282–289.
[10]. Castellanos, F.X., Di Martino, A., Craddock, R.C., Mehta, A.D., Milham, M.P., 2013. Clinical applications of the functional connectome. NeuroImage 80, 527–540.
[11]. Cherkassky, V.L., Kana, R.K., Keller, T.A., Just, M.A., 2006. Functional connectivity in a baseline resting-state network in autism. NeuroReport 17 (16), 1687–1690.

[12]. Craddock, R.C., Holtzheimer, P.E., Hu, X.P., Mayberg, H.S., 2009. Disease state prediction from resting state functional connectivity. Magn. Reson. Med. 62 (6), 1619–1628.

[13]. Craddock, R.C., James, G., 2012. A whole brain fMRI atlas spatial generated via spatially constrained spectral clustering. Human brain … 33 (8).

[14]. Di Martino, A., et al., 2014. The autism brain imaging data exchange: towards large-scale evaluation of the intrinsic brain architecture in autism. 19 (6), 659–667.

[15]. Fox, M.D., 2010. Clinical applications of resting state functional connectivity. Front. Syst. Neurosci. 4, 19.

[16]. Franco, A.R., Mannell, M.V., Calhoun, V.D., Mayer, A.R., 2013. Impact of analysis methods on the reproducibility and reliability of resting-state networks. Brain Connect. 3 (4), 363–374.

[17]. Haxby, J.V., 2001. Distributed and overlapping representations of faces and objects in ventral temporal cortex. Science 293 (5539), 2425–2430.

[18]. Heinsfeld, A.S., Franco, A., Buchweitz, A., Meneguzzi, F., 2017. lsa-pucrs/acerta-abide: Code companion to Neuroimage: Clinical Submission.

[19]. Hjelm, R.D., et al., 2014. Restricted Boltzmann machines for neuroimaging: an application in identifying intrinsic networks. NeuroImage 96, 245–260.

[20]. Ho, T.K., 1995. Random decision forests. In: Document Analysis and Recognition, 1995., Proceedings of the Third International Conference on. 1. pp. 278–282.

[21]. Jordan, M.I., Mitchell, T.M., 2015. Machine learning: trends, perspectives, and prospects. 349 (6245).

[22]. Just, M.A., 2004. Cortical activation and synchronization during sentence comprehension in high-functioning autism: evidence of underconnectivity. Brain 127 (8), 1811–1821.

[23]. Just, M.A., Cherkassky, V.L., Buchweitz, A., Keller, T.A., Mitchell, T.M., 2014. Identifying autism from neural representations of social interactions: neurocognitive markers of autism. PLoS ONE 9 (12), 1–22.

[24]. Just, M.A., Cherkassky, V.L., Keller, T.A., Kana, R.K., Minshew, N.J., 2006. Functional and anatomical cortical underconnectivity in autism: evidence from an fMRI study of an executive function task and corpus callosum morphometry. Cereb. Cortex 17 (4), 951–961.

[25]. Just, M.A., Keller, T.A., Kana, R.K., 2013. A theory of autism based on frontal-posterior underconnectivity. In: Development and Brain Systems in Autism. Psycologicy Press, New York, pp. 35–63.

[26]. Kana, R.K., Keller, T. a., Cherkassky, V.L., Minshew, N.J., Just, M.A., 2009. Atypical fronto-posterior synchronization of theroy of mind regions in autism during mental state attribution. Soc. Neurosci. 4 (2), 135–152.

[27]. Kassam, K.S., Markey, A.R., Cherkassky, V.L., Loewenstein, G., Just, M.A., 2013. Identifying emotions on the basis of neural activation. PLoS ONE 8 (6), e66032.

[28]. Koyamada, S., Shikauchi, Y., Nakae, K., Koyama, M., Ishii, S., 2015. Deep Learning of fMRI Big Data: A Novel Approach to Subject-Transfer Decoding.

[29]. Maaten, L.V.D., Hinton, G., van der Maaten, L.H.G., 2008. Visualizing data using t-SNE. J. Mach. Learn. Res. 9, 2579–2605.

[30]. Mitchell, T.M., et al., 2008. Predicting human brain activity associated with the meanings of nouns. Science 320 (5880), 1191–1195.

[31]. Nielsen, J.A., et al., 2013. Multisite functional connectivity MRI classification of autism: ABIDE results. Front. Hum. Neurosci. 7 (September), 1–12.

[32]. O'Toole, A.J., Jiang, F., Abdi, H., Haxby, J.V., 2005. Partially distributed representations of objects and faces in ventral temporal cortex. J. Cogn. Neurosci. 17 (4), 580–590.

[33]. Pereira, F., Mitchell, T., Botvinick, M., 2009. Machine learning classifiers and fMRI: a tutorial overview. NeuroImage 45 (1), S199–S209.

[34]. Plis, S.M., et al., 2014. Deep learning for neuroimaging: a validation study. Front. Neurosci. 8 (August), 229.

[35]. Plitt, M., Barnes, K.A., Martin, A., 2015. Functional connectivity classification of autism identifies highly predictive brain features but falls short of biomarker standards. NeuroImage: Clinical 7, 359–366.

[36]. Schipul, S.E., Williams, D.L., Keller, T.A., Minshew, N.J., Just, M.A., 2012. Distinctive neural processes during learning in autism. Cereb. Cortex 22 (4), 937–950.

[37]. Shehzad, Z., et al., 2009. The resting brain: unconstrained yet reliable. Cereb. Cortex 19 (10), 2209–2229.

[38]. Shinkareva, S.V., Malave, V.L., Mason, R.A., Mitchell, T.M., Just, M.A., 2011. Commonality of neural representations of words and pictures. NeuroImage 54 (3), 2418–2425.

[39]. Shirer, W.R., Ryali, S., Rykhlevskaia, E., Menon, V., Greicius, M.D., 2012. Decoding subject-driven cognitive states with whole-brain connectivity patterns. Cereb. Cortex 22 (1), 158–165.

[40]. Smith, S.M., et al., 2009. Correspondence of the brain's functional architecture during activation and rest. Proc. Natl. Acad. Sci. 106 (31), 13040–13045.

[41]. Uddin, L.Q., Supekar, K., Menon, V., 2013. Reconceptualizing functional brain connectivity in autism from a developmental perspective. Front. Hum. Neurosci. 7.

[42]. Vapnik, V., 1998. The support vector method of function estimation. In: Nonlinear Modeling. Springer, pp. 55–85. Varoquaux, G., Thirion, B., 2014. How machine learning is shaping cognitive neuroimaging. GigaScience 3 (1), 28.

[43]. Vincent, P., Larochelle, H., Bengio, Y., Manzagol, P.-A., 2008. Extracting and composing robust features with denoising autoencoders. In: Proceedings of the 25th International Conference on Machine Learning, pp. 1096–1103.

[44]. Vincent, P., Larochelle, H., Lajoie, I., Bengio, Y., Manzagol, P.-A., 2010. Stacked denoising autoencoders: learning useful representations in a deep network with a local denoising criterion. J. Mach. Learn. Res. 11 (3), 3371–3408.

[45]. Yang, J., et al., 2010. Common SNPs explain a large proportion of the heritability for human height. Nat. Genet. 42 (7), 565–569.

[46]. Zablotsky, B., Black, L.I., Maenner, M.J., Schieve, L.A., Blumberg, S.J., 2015. Estimated prevalence of autism and other developmental disabilities following questionnaire changes in the 2014 National Health Interview Survey. Natl. Health Stat. Rep. (87), 1–20.